Mathematical Biosciences and Engineering

http://www.aimspress.com/journal/mbe

MBE, 20(4): 7273–7297.
DOI: 10.3934/mbe.2023315
Received: 07 November 2022
Revised: 12 January 2023
Accepted: 30 January 2023
Published: 13 February 2023

Research article

Sliding mode dynamics and optimal control for HIV model

Dan Shi[1], **Shuo Ma**[1,*] **and Qimin Zhang**[1,2,*]

[1] School of Mathematics and Information Science, North Minzu University, Yinchuan 750021, China
[2] School of Mathematics and Statistics, Ningxia University, Yinchuan 750021, China

* **Correspondence:** Email: shuoma@nun.edu.cn, zhangqimin64@sina.com.

Abstract: Considering the drug treatment strategy in both virus-to-cell and cell-to-cell transmissions, this paper presents an HIV model with Filippov control. Given the threshold level N_t, when the total number of infected cells is less or greater than threshold level N_t, the threshold dynamics of the model are studied by using the Routh-Hurwitz Criterion. When the total number of infected cells is equal to N_t, the sliding mode equations are obtained by Utkin equivalent control method, and the dynamics are studied. In addition, the optimal control strategy is introduced for the case that the number of infected cells is greater than N_t. By dynamic programming, the Hamilton-Jacobi-Bellman (HJB) equation is constructed, and the optimal control is obtained. Numerical simulations are presented to illustrate the validity of our results.

Keywords: threshold level; HIV model; sliding mode dynamics; cell-to-cell transmission; optimal control

1. Introduction

Human immunodeficiency virus (HIV) takes the most important $CD4^+T$ lymphocytes in the human immune system as the main target, destroys people's $CD4^+T$ and makes the body lose its immune function [1]. HIV is a major problem facing the human race and poses a serious health threat to human society. While there has been remarkable advancement in the development of antiretroviral therapy (ART) and prevention strategies, currently there are still many people living with HIV [2]. From the National Health Commission of the People's Republic of China, to the end of 2020, a total of 1.053 million people in China were infected with HIV, 351,000 deaths were reported, and the number of infections is expected to increase to 1.6 million in 2022. Therefore, it is beneficial to study the effective control measures and find the optimal control by using mathematical models.

Early HIV models were primarily devoted to the virus-to-cell infection [3–10]. With the development of science and the improvement of medical standards, some studies show that virus can

also spread by direct cell-to-cell transmission [11–15]. Thus, many researchers have begun working on an HIV model incorporating virus-to-cell and cell-to-cell transmission [16–20]. For example, by an HIV model, Wang et al. [16] showed the existence, positivity and boundedness of the model solution. Lai et al. [19] demonstrated global threshold dynamics by the basic reproduction number. For the control of acquired immune deficiency syndrome (AIDS), the main drug treatment is to prevent new HIV infections by blocking the transformation of viral RNA into DNA in T cells and reducing the number of viral particles [21]. With regard to AIDS control, there have already been some results [22–24]. Liu et al. [22], Akbari et al. [23] and Guo et al. [24] proposed an optimal control problem for an HIV infection model with cell-to-cell spread. However, these studies were focused on optimal control given over the entire infection period T, which will increase the cost of control measures. If threshold level N_t can be introduced, such that the control measures are not implemented when the total number of infected cells in an infected person is at a relatively low level (threshold level N_t), while otherwise effective measures are taken to suppress progression of viruses and infected cells, the time and cost will be reduced. The idea has been widely used in engineering [25, 26], but little research has been done in epidemic diseases.

In addition, for the case that the number of infected cells in the body exceeds the threshold level (N_t), from the perspectives of epidemiology and economics, how to control the spread of virus is a valuable question. As indicated by discussion above, in this paper, we analyze the sliding mode dynamics and optimal control of the HIV model with virus-to-cell and cell-to-cell transmission. Here, because the timing of controlling infected cells and viruses is uncertain, dynamic programming is considered, which demonstrates that not only can infected cells and viruses be controlled in time, but also the goal of minimizing the concentration of infected cells and viruses with a low cost of application control can be achieved. The main novelties are summarized as follows:

- About the HIV model with cell-to-cell transmission, the majority of the existing results only discussed dynamics, this article proposes a piecewise control function concerning threshold policy and discusses sliding mode dynamics.
- Differently from previous works on optimal control over the time period $[0, T]$ for the HIV model, in this paper, optimal control strategies for infected cells and viruses are achieved when the total number of infected cells in the body exceeds the certain tolerance threshold level (N_t). Moreover, our results generalize and improve some published results in the literature, such as [23, 24].

The whole organization of this work is as follows. Section 2 describes the different components of the HIV model, and it then further extends a new three-dimensional Filippov model with two control measures. Section 3 investigates the sliding mode dynamics of the model and shows the existence of a unique positive pseudo-equilibrium. In Section 4, the optimal control problem is discussed. We first give the objective function and prove the uniqueness and existence of the viscosity solution of the HJB equation, and we then obtain the optimal control through the Hamiltonian function. The theoretical results are verified by numerical simulations in Section 5. Finally, conclusions and outlook for further work are given in Section 6.

2. Model and preliminary knowledge

Inspired by [17, 19], the classical HIV model with virus-to-cell and cell-to-cell transmission is

$$\begin{cases} \dfrac{dx(t)}{dt} = \Lambda - \beta x(t)v(t) - \gamma x(t)y(t) - ax(t), \\ \dfrac{dy(t)}{dt} = \beta x(t)v(t) + \gamma x(t)y(t) - by(t), \\ \dfrac{dv(t)}{dt} = ky(t) - cv(t), \end{cases} \tag{2.1}$$

where $x(t)$ denotes the concentration of uninfected target cells at time t, $y(t)$ is the concentration of infected cells at time t, and $v(t)$ denotes the concentration of virus particles at time t. Λ is the recruitment rate of healthy target cells, β is the rate at which an uninfected cell becomes infected by an infectious virus, γ represents the infection rate of productively infected cells, k shows the generation rate of virus particles, a expresses the loss rate of infected cells, b represents the natural death rate of uninfected cells, and c indicates the clearance rate of virions.

Based on the existing HIV models, we give the sliding control system to maintain the number of viruses and infected cells below the threshold level. Research [27] has found that current drug treatment consisting of five antiretroviral drugs can suppress viral replication to a low level or increase the CD4+T cell, the two main types of HIV resistance: reverse transcriptase inhibitors (RTIs) and protease inhibitors (PIs) [28, 29]. RTIs prevent new HIV infections by blocking the transformation of viral RNA into DNA in T cells, and PIs reduce the number of viral particles produced by actively infected T cells [21]. We represent by μ_1 the RTIs control variable and by μ_2 the PIs control variable. The control system is given as follows:

$$\begin{cases} \dfrac{dx(t)}{dt} = \Lambda - \beta x(t)v(t) - \gamma x(t)y(t) - ax(t), \\ \dfrac{dy(t)}{dt} = \beta x(t)v(t) + \gamma x(t)y(t) - by(t) - \varepsilon\mu_1 y(t), \\ \dfrac{dv(t)}{dt} = ky(t) - cv(t) - \varepsilon\mu_2 v(t), \end{cases} \tag{2.2}$$

with

$$\varepsilon = \begin{cases} 0, \ y(t) - N_t < 0, \\ 1, \ y(t) - N_t > 0. \end{cases} \tag{2.3}$$

μ_1 is the culling rate of infected cells, μ_2 is the clearance rate of virus particles, and they are constants. The critical level of the total number of infected cells is represented by N_t. For convenience, $y(t) - N_t$ is defined as $\omega(M) = y(t) - N_t$ with vector $M = (x(t), y(t), v(t))^\top \in \mathbb{R}^3_+$ and $\mathbb{R}^3_+ = \{M = (x, y, v) | x \geq 0, y \geq 0, v \geq 0\}$.

Remark 2.1. When $\varepsilon = 0$, model (2.2) becomes model (2.1) and the control measures are taken when $\varepsilon = 1$.

3. The sliding mode dynamics of HIV model

In this section, according to system (2.2) with (2.3), we study the dynamics of the system. First, we define $G_1 = \{M \in \mathbb{R}^3_+ | \omega(M) < 0\}$, $G_2 = \{M \in \mathbb{R}^3_+ | \omega(M) > 0\}$. Furthermore, we describe the manifold G_s as $G_s = \{M \in \mathbb{R}^3_+ | \omega(M) = 0\}$ and the normal vector perpendicular to G_s is shown as $n = (0, 1, 0)^\top$. Then, we consider the following Filippov system:

$$\dot{M} = \begin{cases} f_1(M), & M \in G_1, \\ f_2(M), & M \in G_2, \end{cases} \tag{3.1}$$

where

$$f_1(M) = \begin{pmatrix} \Lambda - ax(t) - \beta x(t)v(t) - \gamma x(t)y(t) \\ \beta x(t)v(t) + \gamma x(t)y(t) - by(t) \\ ky(t) - cv(t) \end{pmatrix},$$

$$f_2(M) = \begin{pmatrix} \Lambda - ax(t) - \beta x(t)v(t) - \gamma x(t)y(t) \\ \beta x(t)v(t) + \gamma x(t)y(t) - by(t) - \mu_1 y(t) \\ ky(t) - cv(t) - \mu_2 v(t) \end{pmatrix}.$$

Based on this, we present the following definitions of various equilibriums and sliding domain.

Definition 3.1. [30] If $f_1(M^*) = 0$ with $\omega(M^*) < 0$, or $f_2(M^*) = 0$ with $\omega(M^*) > 0$, the point M^* is called a real equilibrium of system (3.1).

Definition 3.2. [30] If $f_1(M^*) = 0$ with $\omega(M^*) > 0$, or $f_2(M^*) = 0$ with $\omega(M^*) < 0$, the point M^* is called a virtual equilibrium of system (3.1).

Definition 3.3. [30] If it is an equilibrium of the sliding mode of system (3.1), the point M^* is called a pseudo-equilibrium.

Definition 3.4. [30] S is the sliding domain, if $\langle n, f_1 \rangle > 0$ and $\langle n, f_2 \rangle < 0$ on $S \subset G_s$.

3.1. Analysis in region G_1

In this subsection, we calculate the basic reproduction number and analyze the stability of equilibrium. The dynamics of system (3.1) in region G_1 are indicated by

$$\begin{pmatrix} x'(t) \\ y'(t) \\ v'(t) \end{pmatrix} = \begin{pmatrix} \Lambda - ax(t) - \beta x(t)v(t) - \gamma x(t)y(t) \\ \beta x(t)v(t) + \gamma x(t)y(t) - by(t) \\ ky(t) - cv(t) \end{pmatrix}. \tag{3.2}$$

In subsystem (3.2), the disease-free equilibrium $E_1^0 = \left(\frac{\Lambda}{a}, 0, 0\right)$ and the endemic equilibrium $E_1^* =$

(x_1^*, y_1^*, v_1^*) are given, where

$$\begin{aligned} x_1^* &= \frac{bc}{k\beta + c\gamma}, \\ y_1^* &= \frac{\Lambda(k\beta + c\gamma) - acb}{b(k\beta + c\gamma)}, \\ v_1^* &= \frac{\Lambda k(k\beta + c\gamma) - ackb}{bc(k\beta + c\gamma)}, \\ R_{01} &= \frac{\Lambda(\beta k + c\gamma)}{acb}. \end{aligned}$$

Next, the following theorem about the local asymptotic stability of equilibria E_1^0 and E_1^* are given.

Theorem 3.5. *The disease-free equilibrium E_1^0 is locally asymptotically stable if $R_{01} < 1$; the endemic equilibrium E_1^* exists and is locally asymptotically stable if $R_{01} > 1$.*

Proof. Using the next generation matrix, the basic reproduction number R_{01} of system (3.2) can be deduced, and system (3.2) can be represented as

$$M' = F(M) - V(M),$$

where

$$F(M) = \begin{bmatrix} \beta x(t)v(t) + \gamma x(t)y(t) \\ 0 \\ 0 \end{bmatrix}, V(M) = \begin{bmatrix} by(t) \\ cv(t) - ky(t) \\ ax(t) + \beta x(t)v(t) + \gamma x(t)y(t) - \Lambda \end{bmatrix}.$$

The Jacobian matrix of $F(M)$ and $V(M)$ at the equilibrium point E_1^0 is

$$DF(E_1^0) = \begin{bmatrix} \gamma\frac{\Lambda}{a} & \beta\frac{\Lambda}{a} & 0 \\ 0 & 0 & 0 \\ 0 & 0 & 0 \end{bmatrix}, DV(E_1^0) = \begin{bmatrix} b & 0 & 0 \\ -k & c & 0 \\ \gamma\frac{\Lambda}{a} & \beta\frac{\Lambda}{a} & a \end{bmatrix},$$

where

$$F = \begin{bmatrix} \gamma\frac{\Lambda}{a} & \beta\frac{\Lambda}{a} \\ 0 & 0 \end{bmatrix}, V = \begin{bmatrix} b & 0 \\ -k & c \end{bmatrix}.$$

Then, the generation matrix of system (3.2) is

$$FV^{-1} = \begin{bmatrix} \frac{\Lambda(\beta k + c\gamma)}{acb} & \frac{\beta\Lambda}{ac} \\ 0 & 0 \end{bmatrix}.$$

So, the spectral radius of FV^{-1} is

$$\rho(FV^{-1}) = \frac{\Lambda(\beta k + c\gamma)}{acb},$$

where ρ is the spectral radius of a matrix. Therefore, the basic reproduction number of system (3.2) is

$$R_{01} = \frac{\Lambda(\beta k + c\gamma)}{acb}.$$

For subsystem (3.2), The Jacobian matrix is

$$J_1(x(t), y(t), v(t)) = \begin{pmatrix} -a - \beta v(t) - \gamma y(t) & -\gamma x(t) & -\beta x(t) \\ \beta v(t) + \gamma y(t) & -b + \gamma x(t) & \beta x(t) \\ 0 & k & -c \end{pmatrix}.$$

If $R_{01} < 1$, $cb - \frac{c\gamma\Lambda + k\beta\Lambda}{a} > 0$, $c + b - \frac{\gamma\Lambda}{a} > 0$ can be obtained, and $(c + b - \frac{\gamma\Lambda}{a})^2 - 4(cb - \frac{c\gamma\Lambda + k\beta\Lambda}{a}) > 0$. The characteristic equation at E_1^0 is

$$(\lambda + a)[(\lambda + b - \frac{\gamma\Lambda}{a})(\lambda + c) - \frac{k\beta\Lambda}{a}] = 0,$$

which indicates that

$$\begin{aligned} \lambda_1 &= -a < 0, \\ \lambda_2 &= \frac{-(c + b - \frac{\gamma\Lambda}{a}) + \sqrt{(c + b - \frac{\gamma\Lambda}{a})^2 - 4(cb - \frac{c\gamma\Lambda + k\beta\Lambda}{a})}}{2} < 0, \\ \lambda_3 &= \frac{-(c + b - \frac{\gamma\Lambda}{a}) - \sqrt{(c + b - \frac{\gamma\Lambda}{a})^2 - 4(cb - \frac{c\gamma\Lambda + k\beta\Lambda}{a})}}{2} < 0. \end{aligned}$$

Thus, the eigenvalues of $J(E_1^0)$ are negative when $R_{01} < 1$, so we can obtain that E_1^0 is locally asymptotically stable.

If $R_{01} > 1$, then $\frac{\gamma c\Lambda + k\beta\Lambda}{acb} > 1$, and there exists the endemic equilibrium E_1^*. Thus, the characteristic equation at E_1^* is

$$\lambda^3 + a_1\lambda^2 + a_2\lambda + a_3 = 0,$$

where

$$\begin{aligned} a_1 &= a + c + b + \beta v_1^* + \gamma y_1^* - \gamma x_1^* \\ &= a + c + b + \beta\frac{\Lambda k(k\beta + c\gamma) - ackb}{bc(k\beta + c\gamma)} + \gamma\frac{\Lambda(k\beta + c\gamma) - acb}{b(k\beta + c\gamma)} - \gamma\frac{bc}{k\beta + c\gamma} \\ &= c + a + \frac{bk\beta}{k\beta + c\gamma} > 0, \\ a_2 &= bc + ac + ab - (\gamma c + k\beta + a\gamma)x_1^* + (c\beta + b\beta)v_1^* + (c\gamma + b\gamma)y_1^* \\ &= bc + ac + ab - (\gamma c + k\beta + a\gamma)\frac{bc}{k\beta + c\gamma} + (c\beta + b\beta)\frac{\Lambda k(k\beta + c\gamma) - ackb}{bc(k\beta + c\gamma)} \\ &\quad + (c\gamma + b\gamma)\frac{\Lambda(k\beta + c\gamma) - acb}{b(k\beta + c\gamma)} \\ &= ca + \frac{akb\beta}{k\beta + c\gamma} > 0, \\ a_3 &= acb - (ac\gamma + ak\beta)x_1^* + bc\beta v_1^* + bc\gamma y_1^* \\ &= acb - (ac\gamma + ak\beta)\frac{bc}{k\beta + c\gamma} + bc\beta\frac{\Lambda k(k\beta + c\gamma) - ackb}{bc(k\beta + c\gamma)} + bc\gamma\frac{\Lambda(k\beta + c\gamma) - acb}{b(k\beta + c\gamma)} \\ &= \Lambda(k\beta + c\gamma) - acb > 0. \end{aligned}$$

Moreover, we can get

$$\begin{aligned}
a_1a_2 - a_3 &= [a + c + b + \beta v_1^* + \gamma y_1^* - \gamma x_1^*][bc + ac + ab - (\gamma c + k\beta + a\gamma)x_1^* + (c\beta + b\beta)v_1^* \\
&\quad + (c\gamma + b\gamma)y_1^*] - [acb - (ac\gamma + ak\beta)x_1^* + bc\beta v_1^* + bc\gamma y_1^*] \\
&= \frac{\Lambda(k\beta + c\gamma) - acb}{bc(k\beta + c\gamma)}[bbk\beta + akb\beta + acc\gamma + bck\beta + cck\beta + ccc\gamma + cak\beta + cac\gamma] \\
&\quad + (cak\beta + cac\gamma + abk\beta)\frac{bk\beta + ck\beta + cc\gamma + ak\beta + ac\gamma}{(k\beta + c\gamma)^2} \\
&\quad + 2k\beta\gamma(b + c)\frac{\Lambda(k\beta + c\gamma) - acb}{bc(k\beta + c\gamma)} \cdot \frac{\Lambda(k\beta + c\gamma) - acb}{b(k\beta + c\gamma)} \\
&\quad + \frac{\Lambda(k\beta + c\gamma) - acb}{bc(k\beta + c\gamma)}(ack\beta + cac\gamma + akb\beta) \\
&> 0.
\end{aligned}$$

According to the Routh-Hurwitz Criterion, all eigenvalues of $J(E_1^*)$ have negative real parts. Hence, this represents that E_1^* is locally asymptotic stable.

3.2. Analysis in region G_2

In region G_2, we give the dynamics of system (3.1):

$$\begin{pmatrix} x'(t) \\ y'(t) \\ v'(t) \end{pmatrix} = \begin{pmatrix} \Lambda - ax(t) - \beta x(t)v(t) - \gamma x(t)y(t) \\ \beta x(t)v(t) + \gamma x(t)y(t) - by(t) - \mu_1 y(t) \\ ky(t) - cv(t) - \mu_2 v(t) \end{pmatrix}. \tag{3.3}$$

In subsystem (3.3), the disease-free equilibrium $E_2^0 = \left(\frac{\Lambda}{a}, 0, 0\right)$ and the endemic equilibrium $E_2^* = (x_2^*, y_2^*, v_2^*)$ are given, where

$$\begin{aligned}
x_2^* &= \frac{(c + \mu_2)(b + \mu_1)}{k\beta + \gamma(c + \mu_2)}, \\
y_2^* &= \frac{\Lambda}{b + \mu_1} - \frac{a(c + \mu_2)}{k\beta + \gamma(c + \mu_2)}, \\
v_2^* &= \frac{k\Lambda}{(c + \mu_2)(b + \mu_1)} - \frac{ak}{k\beta + \gamma(c + \mu_2)}, \\
R_{02} &= \frac{\Lambda(k\beta + \gamma(c + \mu_2))}{a(c + \mu_2)(b + \mu_1)}.
\end{aligned}$$

Next, the following theorem about the local asymptotic stability of equilibria E_2^0 and E_2^* are given.

Theorem 3.6. *The disease-free equilibrium E_2^0 is locally asymptotically stable if $R_{02} < 1$. The endemic equilibrium E_2^* exists and is locally asymptotically stable if $R_{02} > 1$.*

Proof. Using the next generation matrix, we deduce the basic reproduction number R_{02} of system (3.3):

$$\begin{aligned}
R_{02} &= \rho\left(\begin{bmatrix} \gamma\frac{\Lambda}{a} & \beta\frac{\Lambda}{a} \\ 0 & 0 \end{bmatrix}\begin{bmatrix} b + \mu_1 & 0 \\ -k & c + \mu_2 \end{bmatrix}^{-1}\right) \\
&= \frac{\Lambda(k\beta + \gamma(c + \mu_2))}{a(c + \mu_2)(b + \mu_1)}.
\end{aligned}$$

For subsystem (3.3), the Jacobian matrix is

$$J_2(x(t), y(t), v(t)) = \begin{pmatrix} -a - \beta v(t) - \gamma y(t) & -\gamma x(t) & -\beta x(t) \\ \beta v(t) + \gamma y(t) & -b + \gamma x(t) - \mu_1 & \beta x(t) \\ 0 & k & -c - \mu_2 \end{pmatrix}.$$

Let $c + \mu_2 = c_1$, $b + \mu_1 = b_1$. Similar to the proof of Theorem 3.5, if $R_{02} < 1$, then all eigenvalues of $J(E_2^0)$ are negative, and thus the local asymptotic stability of E_2^0 can also be concluded. Furthermore, all eigenvalues of $J(E_2^*)$ have negative real parts, if $R_{02} > 1$, which shows that E_2^* is locally asymptotically stable.

Remark 3.7. The basic reproduction number R_{02} is related to control variables μ_1 and μ_2, and when $\mu_1 = \mu_2 = 0$, that is, the control measures are not implemented, we have $R_{01} = R_{02}$.

3.3. Analysis in region G_s

In order to study the dynamics of sliding mode of system (3.1) in this subsection, we initially examine the existence of the sliding mode. The manifold G_s is defined as $y(t) = N_t$, and we have

$$\begin{aligned} \langle n, f_1 \rangle &= \left\langle \begin{pmatrix} 0 \\ 1 \\ 0 \end{pmatrix}, \begin{pmatrix} \Lambda - ax(t) - \beta x(t)v(t) - \gamma x(t)y(t) \\ \beta x(t)v(t) + \gamma x(t)y(t) - by(t) \\ ky(t) - cv(t) \end{pmatrix} \right\rangle \\ &= \beta x(t)v(t) - bN_t + \gamma x(t)N_t \\ &= \sigma_1(x(t), v(t)), \end{aligned} \tag{3.4}$$

and

$$\begin{aligned} \langle n, f_2 \rangle &= \left\langle \begin{pmatrix} 0 \\ 1 \\ 0 \end{pmatrix}, \begin{pmatrix} \Lambda - ax(t) - \beta x(t)v(t) - \gamma x(t)y(t) \\ \beta x(t)v(t) + \gamma x(t)y(t) - by(t) - \mu_1 y(t) \\ ky(t) - cv(t) - \mu_2 v(t) \end{pmatrix} \right\rangle \\ &= \beta x(t)v(t) - bN_t + \gamma x(t)N_t - \mu_1 N_t \\ &= \sigma_2(x(t), v(t)), \end{aligned} \tag{3.5}$$

which shows that $\sigma_2(x(t), v(t)) < \sigma_1(x(t), v(t))$. Because $\langle n, f_1 \rangle > 0$ and $\langle n, f_2 \rangle < 0$, we can obtain

$$\begin{aligned} \langle n, f_1 \rangle > 0, \ if \ x(t) > \frac{bN_t}{\beta v(t) + \gamma N_t} = H_1(v(t)), \\ \langle n, f_2 \rangle < 0, \ if \ x(t) < \frac{bN_t + \mu_1 N_t}{\beta v(t) + \gamma N_t} = H_2(v(t)), \end{aligned}$$

and

$$H_2(v(t)) > H_1(v(t)).$$

It is obvious that $H_1(v(t))$ is positive on the interval $(0, N_t)$, and so is $H_2(v(t))$. Then, the sliding domain $S \subset G_s$ is defined as follows:

$$S \triangleq \{(x(t), y(t), v(t)) \in G_s : H_1(v(t)) < x(t) < H_2(v(t)), y(t) = N_t\}. \tag{3.6}$$

Moreover, in order to obtain sliding mode equations in the region S, we use the Utkin equivalent control method, as used in [31]. First, according to $\omega(y(t)) = y(t) - N_t = 0$ and $d\omega/dt = 0$,

$$\begin{aligned}\frac{d\omega}{dt} &= \frac{\partial\omega}{\partial y(t)}\frac{dy(t)}{dt}\\ &= \beta x(t)v(t) - by(t) + \gamma x(t)y(t) - \varepsilon\mu_1 y(t)\\ &= 0.\end{aligned} \tag{3.7}$$

By solving Eq (3.7), the function about ε is obtained:

$$\begin{aligned}\varepsilon(v(t)) &= \frac{\beta x(t)v(t) - by(t) + \gamma x(t)y(t)}{\mu_1 y(t)}\\ &= \frac{\beta x(t)v(t) - bN_t + \gamma x(t)N_t}{\mu_1 N_t}.\end{aligned} \tag{3.8}$$

Substitute Eq (3.8) into system (2.2), and the dynamics of sliding mode in S can be given by differential equations as follows:

$$\begin{cases}\dfrac{dx(t)}{dt} = \Lambda - ax(t) - \beta x(t)v(t) - \gamma x(t)N_t,\\ \dfrac{dy(t)}{dt} = 0,\\ \dfrac{dv(t)}{dt} = \dfrac{k\mu_1 N_t^2 - c\mu_1 N_t v(t) + b\mu_2 N_t v(t) - \gamma\mu_2 N_t x(t)v(t) - \mu_2\beta x(t)v^2(t)}{\mu_1 N_t}.\end{cases} \tag{3.9}$$

Next, we exhibit the following proposition about the existence of equilibrium of sliding mode (3.9).

Proposition 3.8. *The existence of a unique positive pseudo-equilibrium* $E_s^* = (\frac{\Lambda}{a+\beta v^*+\gamma N_t}, N_t, v^*)$ *of sliding mode* (3.9) *is obtained if* $\frac{c-k}{b} < \frac{\mu_2}{\mu_1} < \frac{c}{b}$ *and* $E_s^* \in S$.

Proof. Let $\frac{dx(t)}{dt} = 0$ and $\frac{dv(t)}{dt} = 0$. It obtains that

$$x(t) = \frac{\Lambda}{a + \beta v(t) + \gamma N_t}, \tag{3.10}$$

and

$$k\mu_1 N_t^2 - c\mu_1 N_t v(t) + b\mu_2 N_t v(t) - \gamma\mu_2 N_t x(t)v(t) - \mu_2\beta x(t)v^2(t) = 0. \tag{3.11}$$

After substituting Eq (3.10) into (3.11), we get the following equation of $v(t)$:

$$\tau_1 v^2(t) + \tau_2 v(t) + \tau_3 = 0, \tag{3.12}$$

where

$$\begin{aligned}\tau_1 &= \beta N_t(b\mu_2 - c\mu_1) - \mu_2\beta\Lambda,\\ \tau_2 &= ab\mu_2 N_t - ca\mu_1 N_t - \gamma\Lambda\mu_2 N_t + b\gamma\mu_2 N_t^2 - c\gamma\mu_1 N_t^2 + k\beta\mu_1 N_t^2,\\ \tau_3 &= ak\mu_1 N_t^2 + k\gamma\mu_1 N_t^3,\\ \Delta &= \tau_2^2 - 4\tau_1\tau_3\\ &= N_t^2[ab\mu_2 - ca\mu_1 - \gamma\Lambda\mu_2 + b\gamma\mu_2 N_t - c\gamma\mu_1 N_t + k\beta\mu_1 N_t]^2\\ &\quad - 4(\beta N_t(b\mu_2 - c\mu_1) - \mu_2\beta\Lambda)[ak\mu_1 N_t^2 + k\gamma\mu_1 N_t^3].\end{aligned}$$

If $\frac{c-k}{b} < \frac{\mu_2}{\mu_1} < \frac{c}{b}$, then $\tau_1 < 0, \tau_3 > 0$ and $\Delta > 0$ can be received. The Vieta Theorem shows

$$v_1^* v_2^* = \frac{\tau_3}{\tau_1} < 0. \tag{3.13}$$

Due to $\Delta > 0$, the existence of the root is proven, and there are two roots, one positive root and one negative root from (3.13). We can conclude that Eq (3.12) has a unique positive root denoted by v^*. Thus, the equilibrium point E_s^* can be obtained from (3.10):

$$E_s^* = (x^*, y^*, v^*) = \left(\frac{\Lambda}{a + \beta v^* + \gamma N_t}, N_t, v^* \right).$$

Furthermore, E_s^* is a unique pseudo-equilibrium if $E_s^* \in S \subset G_s$ holds.

Similar to the previous theorem, it is worth considering the local asymptotical stability of E_s^*, and then the following theorem is given.

Theorem 3.9. *Under the same conditions of Proposition 3.8, E_s^* is locally asymptotically stable on the sliding domain S.*

Proof. In system (3.9), the Jacobian matrix of the first two equations is

$$\mathbf{J}_s(x^*, v^*) = \begin{pmatrix} J_{11} & J_{12} \\ J_{21} & J_{22} \end{pmatrix}. \tag{3.14}$$

From Proposition 3.8, $\frac{c-k}{b} < \frac{\mu_2}{\mu_1} < \frac{c}{b}$, we set

$$\begin{aligned} P &= \frac{dx(t)}{dt} = \Lambda - ax(t) - \beta x(t)v(t) - \gamma x(t)N_t, \\ Q &= \frac{dv(t)}{dt} = \frac{k\mu_1 N_t^2 - c\mu_1 N_t v(t) + b\mu_2 N_t v(t) - \gamma\mu_2 N_t x(t)v(t) - \mu_2 \beta x(t)v^2(t)}{\mu_1 N_t}, \end{aligned} \tag{3.15}$$

and obtain

$$\begin{aligned} J_{11} &= \left.\frac{\partial P}{\partial x}\right|_{(x^*,v^*)} = -a - \beta v^* - \gamma N_t < 0, \\ J_{12} &= \left.\frac{\partial P}{\partial v}\right|_{(x^*,v^*)} = -\beta x^* < 0, \\ J_{21} &= \left.\frac{\partial Q}{\partial x}\right|_{(x^*,v^*)} = \frac{-\gamma\mu_2 v^* N_t - \mu_2\beta(v^*)^2}{\mu_1 N_t} < 0, \\ J_{22} &= \left.\frac{\partial Q}{\partial v}\right|_{(x^*,v^*)} = \frac{-c\mu_1 N_t + b\mu_2 N_t - \gamma\mu_2 N_t x^* - 2\mu_2\beta x^* v^*}{\mu_1 N_t} < 0. \end{aligned} \tag{3.16}$$

Thus, we get

$$J_{11} \cdot J_{22} - J_{12} \cdot J_{21} > 0, \tag{3.17}$$

since $J_{11} + J_{22} < 0$, and we can obtain that

$$\begin{aligned} & J_{11} \cdot J_{22} - J_{12} \cdot J_{21} \\ &= [-a - \beta v^* - \gamma N_t] \cdot \frac{-c\mu_1 N_t + b\mu_2 N_t - \gamma\mu_2 N_t x^* - 2\mu_2\beta x^* v^*}{\mu_1 N_t} - (-\beta x^*) \cdot \frac{-\gamma\mu_2 v^* N_t - \mu_2\beta(v^*)^2}{\mu_1 N_t} \\ &= \frac{(a + \beta v^* + \gamma N_t) \cdot (c\mu_1 N_t - b\mu_2 N_t) + (a + \gamma N_t)\gamma\mu_2 N_t x^* + (a + \beta v^* + \gamma N_t)\mu_2\beta x^* v^*}{\mu_1 N_t} > 0. \end{aligned} \tag{3.18}$$

Therefore, all eigenvalues of (3.14) have negative real parts. That E_s^* is locally asymptotically stable can be obtained easily.

Remark 3.10. The sliding domain S represents the region between the two lines associated with $x(t), v(t)$ belonging to the plane $y = N_t$, and the local asymptotical stability of pseudo-equilibrium E_s^* in sliding domain S is related to the control variables, which needs to satisfy the condition of the parameters.

4. Optimal control problem

In order to reduce the number of infected cells and viruses, while keeping the cost to apply the control at the minimum level at any time, we show an optimal control problem on the basis of system (2.2). In this section, any time refers to when the number of infected cells is greater than threshold level N_t, that is, when $\varepsilon = 1$ in system (2.2). If the control variable in system (2.2) is a time dependent variable, how do we find the optimal control? Thus, we represent by $u_1(t)$ the RTIs control variable and by $u_2(t)$ the PIs control variable. First, we have $u(t) = (u_1(t), u_2(t))^\top \in \mathcal{V}[s, T] = \{u(\cdot) : [s, T] \to U |\ u_1(t)$ *and* $u_2(t)$ *are measurable* $: 0 \le u_1(t) \le 1, 0 \le u_2(t) \le 1\}$, where U is a metric space and convex, $T > 0$, and the control problem of the model is given by

$$\begin{cases} \dfrac{dx(t)}{dt} = \Lambda - \beta x(t)v(t) - \gamma x(t)y(t) - ax(t), \\ \dfrac{dy(t)}{dt} = \beta x(t)v(t) + \gamma x(t)y(t) - by(t) - u_1(t)y(t), \qquad t > 0, \\ \dfrac{dv(t)}{dt} = ky(t) - cv(t) - u_2(t)v(t). \end{cases} \tag{4.1}$$

Let $(s, M) \in [0, T) \times \mathbb{R}^3$, and we consider the following control system over $[s, T]$:

$$\begin{cases} \dfrac{dM(t)}{dt} = b(t, M(t), u(t)), \qquad t \in [s, T], \\ M(s) = M_0, \end{cases} \tag{4.2}$$

where $M(t) = (x(t), y(t), v(t))^\top \in \mathbb{R}^3$. Next, we construct the following objective functional:

$$J(u_1(t), u_2(t)) = \int_s^T (A_1 u_1^2(t) + A_2 u_2^2(t) + A_3 y(t) + A_4 v(t))dt + h(M(T)), \tag{4.3}$$

where A_i $(i = 1, 2, 3, 4)$ are weights to make the terms of the integrand keep balance. The term $\int_s^T (A_1 u_1^2(t) + A_2 u_2^2(t))dt$ gives the total cost of using the control strategy, $h(M(T))$ is the penalty

function corresponding to the terminal state, and $\int_s^T (A_3 y(t) + A_4 v(t))dt$ represents the total number of infected cells and viruses over the time period T. It is important to find an optimal control pair $(u_1^*(t), u_2^*(t)), t \in [s, T]$ such that

$$J(u_1^*(t), u_2^*(t)) = \min_{u_1(t), u_2(t) \in \mathcal{V}_{[s,T]}} J(u_1(t), u_2(t)). \tag{4.4}$$

Further, the value function is as follows:

$$\begin{cases} V(s, M_0) = \inf\limits_{u_1(t), u_2(t) \in \mathcal{V}_{[s,T]} J(s, M_0; u_1(t), u_2(t))}, & \forall (s, M_0) \in [0, T) \times \mathbb{R}^3, \\ V(T, M_0) = h(M_0), & \forall M_0 \in \mathbb{R}^3. \end{cases} \tag{4.5}$$

Before further study, we give the following assumption.

Assumption 1. $(U, \tilde{d})$ is a separable metric space.

Then, we would like to study $V(\cdot, \cdot)$ in great detail and present the following results called Bellman's principle of optimality by [32].

Theorem 4.1. *Let 1 hold, and U is convex. Then, for any* $(s, M_0) \in [0, T) \times \mathbb{R}^3$*, we have*

$$\begin{aligned} V(s, M_0) = \inf_{u_1(t), u_2(t) \in \mathcal{V}_{[s,T]}} \{ & \int_s^{\hat{s}} (A_1 u_1^2(t) + A_2 u_2^2(t) + A_3 y(t) \\ & + A_4 v(t))dt + V(\hat{s}, M(\hat{s}; s, M_0, u(\cdot)))\}, \qquad \forall 0 \le s \le \hat{s} \le T. \end{aligned} \tag{4.6}$$

Proof. Let us define

$$\bar{V}(s, M_0) = \{ \int_s^{\hat{s}} (A_1 u_1^2(t) + A_2 u_2^2(t) + A_3 y(t) + A_4 v(t))dt + V(\hat{s}, M(\hat{s}; s, M_0, u(\cdot)))\}. \tag{4.7}$$

By (4.6), we obtain

$$\begin{aligned} \bar{V}(s, M_0) \le J(s, M_0; u(t)) = & \int_s^{\hat{s}} (A_1 u_1^2(t) + A_2 u_2^2(t) + A_3 y(t) + A_4 v(t))dt \\ & + J(\hat{s}, M(\hat{s}); u(\cdot))), \qquad \forall u(t) \in \mathcal{V}[s, T]. \end{aligned} \tag{4.8}$$

Therefore, we take the infimum over $u(t) \in \mathcal{V}[s, T]$ and get

$$V(s, M_0) \le \bar{V}(s, M_0), \tag{4.9}$$

and there exists a $u_\varepsilon(t) \in \mathcal{V}[s, T]$ for $\forall \varepsilon > 0$ such that

$$V(s, M_0) + \varepsilon \ge J(s, M_0; u_\varepsilon(t)) \ge \int_s^{\hat{s}} (A_1 u_1^2(t) + A_2 u_2^2(t) + A_3 y(t) + A_4 v(t))dt + J(\hat{s}, M_\varepsilon(\hat{s})) \ge \bar{V}(s, M_0), \tag{4.10}$$

where $M_\varepsilon(\cdot) = M(\cdot; s, M_0, u_\varepsilon(\cdot))$. Combining (4.9) and (4.10), (4.6) is obvious. This completes the proof.

(4.6) is called the dynamic programming equation, and the equation is difficult to handle. Thus, we construct the Hamilton-Jacobi-Bellman (HJB) equation as follows.

Theorem 4.2. *Let 1 hold, and U is convex. Suppose $V \in C^1([0,T]\times\mathbb{R}^3)$. Then, $V(s,M_0)$ is a solution to the following terminal value problem of a first-order partial differential equation:*

$$\begin{cases} 0 = -V_t + \sup\limits_{u(t)\in U} H(t,M,u(t),-V_M), & (t,M)\in[0,T]\times\mathbb{R}^3,\\ V|_{t=T} = h(M), & M\in\mathbb{R}^3, \end{cases} \tag{4.11}$$

where

$$\begin{aligned} H(t,M,u(t),-V_M) &= -V_x(\Lambda - ax(t) - \beta x(t)v(t) - \gamma x(t)y(t)) - V_y(\beta x(t)v(t) + \gamma x(t)y(t) - by(t)\\ &\quad - u_1(t)y(t)) - V_v(ky(t) - cv(t) - u_2(t)v(t)) - A_1u_1^2(t) - A_2u_2^2(t) - A_3y(t) - A_4v(t). \end{aligned} \tag{4.12}$$

We call (4.11) *the Hamilton-Jacobi-Bellman (HJB) equation associated with* (4.5).

Proof. Fix a $u\in U$. Let $M(t)$ be the state trajectory corresponding to the control $u(t)\equiv u$. According to (4.6) with $\hat{s}\downarrow s$, we get

$$\begin{aligned} 0 \geq & -\frac{V(\hat{s},M(\hat{s}))-V(s,M_0)}{\hat{s}-s} - \frac{1}{\hat{s}-s}\int_s^{\hat{s}}(A_1u_1^2(t)+A_2u_2^2(t)+A_3y(t)+A_4v(t))dt\\ &\to -V_t(s,M_0) - (V_x(\Lambda - ax(t) - \beta x(t)v(t) - \gamma x(t)y(t)) + V_y(\beta x(t)v(t) + \gamma x(t)y(t) - by(t) - u_1(t)y(t))\\ &+ V_v(ky(t) - cv(t) - u_2(t)v(t))) - (A_1u_1^2(t) + A_2u_2^2(t) + A_3y(t) + A_4v(t)), \quad \forall u\in U, \end{aligned} \tag{4.13}$$

which results in

$$\begin{aligned} 0 \geq & -V_t(s,M_0) + \sup_{u\in U}\{-V_x(\Lambda - ax(t) - \beta x(t)v(t) - \gamma x(t)y(t)) - V_y(\beta x(t)v(t) + \gamma x(t)y(t) - by(t)\\ &- u_1(t)y(t)) - V_v(ky(t) - cv(t) - u_2(t)v(t)) - A_1u_1^2(t) - A_2u_2^2(t) - A_3y(t) - A_4v(t)\}. \end{aligned} \tag{4.14}$$

For any $\varepsilon>0$, $0\leq s\leq\hat{s}\leq T$ with $\hat{s}-s>0$ small enough, there exists a $u=u_{\varepsilon,\hat{s}}(\cdot)\in\mathcal{V}[s,T]$ such that

$$V(s,M_0)+\varepsilon(\hat{s}-s) \geq \int_s^{\hat{s}}(A_1u_1^2(t)+A_2u_2^2(t)+A_3y(t)+A_4v(t))dt + V(\hat{s},M(\hat{s})), \tag{4.15}$$

so it follows that

$$\begin{aligned} -\varepsilon \leq & -\frac{V(\hat{s},M(\hat{s}))-V(s,M_0)}{\hat{s}-s} - \frac{1}{\hat{s}-s}\int_s^{\hat{s}}(A_1u_1^2(t)+A_2u_2^2(t)+A_3y(t)+A_4v(t))dt\\ &= \frac{1}{\hat{s}-s}\int_s^{\hat{s}}\{-V_t(t,M) - [V_x(\Lambda - ax(t) - \beta x(t)v(t) - \gamma x(t)y(t)) + V_y(\beta x(t)v(t) + \gamma x(t)y(t)\\ &- by(t) - u_1(t)y(t)) + V_v(ky(t) - cv(t) - u_2(t)v(t))] - [A_1u_1^2(t) + A_2u_2^2(t) + A_3y(t) + A_4v(t)]\}dt\\ &\leq \frac{1}{\hat{s}-s}\int_s^{\hat{s}}\{-V_t(t,M) + \sup_{u\in U}\{-V_x(\Lambda - ax(t) - \beta x(t)v(t) - \gamma x(t)y(t)) - V_y(\beta x(t)v(t) + \gamma x(t)y(t)\\ &- by(t) - u_1(t)y(t)) - V_v(ky(t) - cv(t) - u_2(t)v(t)) - A_1u_1^2(t) - A_2u_2^2(t) - A_3y(t) - A_4v(t)\}\}dt\\ &\to -V_t(s,M_0) + \sup_{u\in U}\{-V_x(\Lambda - ax(t) - \beta x(t)v(t) - \gamma x(t)y(t)) - V_y(\beta x(t)v(t) + \gamma x(t)y(t) - by(t)\\ &- u_1(t)y(t)) - V_v(ky(t) - cv(t) - u_2(t)v(t)) - A_1u_1^2(t) - A_2u_2^2(t) - A_3y(t) - A_4v(t)\}. \end{aligned} \tag{4.16}$$

Combining (4.14) and (4.16), we complete the proof.

For further study, the definition of viscosity solution of (4.11) by [32] is given.

Definition 4.3. A function $V \in C[0,T] \times \mathbb{R}^3)$ is called a viscosity subsolution (or supersolution) of (4.11) if

$$V(T,M) \leq h(M), (V(T,M) \geq h(M)) \quad \forall M \in \mathbb{R}^3, \tag{4.17}$$

and for any $\varphi \in C^1([0,T] \times \mathbb{R})$, whenever $V - \varphi$ attains a local maximum(or minimum) at $(t,M) \in [0,T] \times \mathbb{R}^3$, we have

$$-\varphi_t(t,M) + \sup_{u(t)\in U} H(t,M,u(t),-\varphi_M(T,M)) \leq 0, \ \ (-\varphi_t(t,M) + \sup_{u(t)\in U} H(t,M,u(t),-\varphi_M(T,M)) \geq 0). \tag{4.18}$$

In this case that V is both a viscosity subsolution and supersolution of (4.11), it is a viscosity solution of (4.11).

If we get the value function V by solving the HJB equation, then an optimal pair could be constructed. Thus, the characterization of the value function of the viscosity solution to the HJB equation is given below.

Theorem 4.4. *Let 1 hold, and U is convex. Then, the value function $V(\cdot,\cdot)$ satisfies*

$$|V(s,M_0) - V(\bar{s},\bar{M}_0)| \leq K|s-\bar{s}|, \ \forall (s,M_0),(\bar{s},\bar{M}_0) \in [0,T] \times \mathbb{R}^3, \tag{4.19}$$

for some $K > 0$. Moreover, V is the only viscosity solution of (4.11) *in the class $C([0,T] \times \mathbb{R}^3)$.*

Proof. We have

$$\begin{aligned} |V(s,M_0) - V(\bar{s},\bar{M}_0)| &= |\inf_{u_1,u_2\in\mathcal{V}_{[s,T]}} \int_s^T [A_1u_1^2(t) + A_2u_2^2(t) + A_3y(t) + A_4v(t)]dt \\ &\quad - \inf_{u_1,u_2\in\mathcal{V}_{[s,T]}} \int_{\bar{s}}^T [A_1u_1^2(t) + A_2u_2^2(t) + A_3y(t) + A_4v(t)]dt| \\ &\leq |\int_s^{\bar{s}} [A_1u_1^2(t) + A_2u_2^2(t) + A_3y(t) + A_4v(t)]dt| \\ &\leq K|s-\bar{s}|, \end{aligned} \tag{4.20}$$

where $K = \max\{A_1u_1^2(t) + A_2u_2^2(t) + A_3y(t) + A_4v(t)\} > 0$. Then, similar to [32, Theorem 2.5], the value function V clearly satisfies the condition and is the only viscosity solution of (4.11).

Next, in order to discuss the existence of the optimal control pair, we define $H(t,M,u(t),p)$ as the Hamiltonian as follows:

$$\begin{aligned} H(t,M,u(t),p) &= (\Lambda - ax(t) - \beta x(t)v(t) - \gamma x(t)y(t))p_1 + (\beta x(t)v(t) + \gamma x(t)y(t) - by(t) \\ &\quad - u_1(t)y(t))p_2 + (ky(t) - cv(t) - u_2(t)v(t))p_3 + A_1u_1^2(t) + A_2u_2^2(t) + A_3y(t) + A_4v(t). \end{aligned} \tag{4.21}$$

Theorem 4.5. *There exists an optimal control pair $\left(u_1^*(t), u_2^*(t)\right)$ and a corresponding optimal state $(x^*(t), y^*(t), v^*(t))$ such that*

$$J\left(u_1^*(t), u_2^*(t)\right) = \min_{u_1(t),u_2(t)\in U} J\left(u_1(t), u_2(t)\right). \tag{4.22}$$

Proof. Note that both the control variables and state variables are nonnegative, and the objective functional (4.3) is convex with respect to the control variables. The convexity and closure of the control set U are obtained according to the definition of it. Furthermore, the optimal control is bounded. Therefore, we conclude that there exists an optimal control $u_1^*(t), u_2^*(t)$ for $J\left(u_1^*(t), u_2^*(t)\right) = \min_{u_1(t),u_2(t)\in U} J\left(u_1(t), u_2(t)\right)$.

The HJB equation and the value function have been discussed. Further, we figure out the optimal control as follows.

Theorem 4.6. *Let $u_1^*(t), u_2^*(t)$ be optimal control variables, and $x^*(t), y^*(t), v^*(t)$ are corresponding optimal state variables. There exists adjoint process $p(t) = (p_1(t), p_2(t), p_3(t))^\top$, satisfying the following adjoint equation:*

$$\begin{cases} dp_1(t) = -\left[(-a-\beta v(t)-\gamma y(t))p_1(t) + (\beta v(t)+\gamma y(t))p_2(t)\right]dt \\ dp_2(t) = -\left[(-\gamma x(t))p_1(t) + (\gamma x(t) - b - u_1(t))\,p_2(t) + kp_3(t) + A_3\right]dt \\ dp_3(t) = -\left[(-\beta x)p_1(t) + (\beta x)p_2(t) + (-c-u_2(t))\,p_3(t) + A_4\right]dt \\ p_i(T) = 0, i = 1, 2, 3. \end{cases} \tag{4.23}$$

Furthermore, the optimal control is given as follows:

$$u_i^*(t) = \min\left\{\max\left\{B_i, 0\right\}, 1\right\}, i = 1, 2, \tag{4.24}$$

where $B_1 = \frac{y^*(t)p_2(t)}{2A_1}, B_2 = \frac{v^*(t)p_3(t)}{2A_2}$.

Proof. Because the Hamiltonian function H is given. Moreover, by using the optimal condition, and we obtain $u_1^*(t)$ and $u_2^*(t)$

$$\frac{\partial H}{\partial u_1} = 0, \frac{\partial H}{\partial u_2} = 0. \tag{4.25}$$

Hence,

$$u_1^*(t) = \frac{y^*(t)p_2(t)}{2A_1}, u_2^*(t) = \frac{v^*(t)p_3(t)}{2A_2}. \tag{4.26}$$

So, $B_1 = \frac{y^*(t)p_2(t)}{2A_1}, B_2 = \frac{v^*(t)p_3(t)}{2A_2}$ are taken, and the optimal control $u_1^*(t), u_2^*(t)$ follows:

$$u_1^*(t) = \begin{cases} 0, & \text{if } \frac{y^*(t)p_2(t)}{2A_1} < 0, \\ \frac{y^*(t)p_2(t)}{2A_1}, & \text{if } 0 \le \frac{y^*(t)p_2(t)}{2A_1} \le 1, \\ 1, & \text{if } \frac{y^*(t)p_2(t)}{2A_1} > 1, \end{cases} \quad u_2^*(t) = \begin{cases} 0, & \text{if } \frac{v^*(t)p_3(t)}{2A_2} < 0, \\ \frac{v^*(t)p_3(t)}{2A_2}, & \text{if } 0 \le \frac{v^*(t)p_3(t)}{2A_2} \le 1, \\ 1, & \text{if } \frac{v^*(t)p_3(t)}{2A_2} > 1. \end{cases} \tag{4.27}$$

Thus, the optimal value can be obtained.

Remark 4.7. In practical problems, when the parameters are known, the optimal control $u_1^*(t)$ and $u_2^*(t)$ can be calculated by using computer programming for Eqs (4.1), (4.23) and (4.27), that is, the dosage intensity of RTIs and PIs at each time can be calculated. If patients are treated in such a proportion, an optimal control strategy to minimize the costs and the number of viruses and infected cells can be obtained.

5. Numerical simulations

In this section, several numerical simulations are presented to prove and verify the above theoretical results by MATLAB software.

5.1. Numerical simulations of sliding mode

In this subsection, numerical simulations are performed to illustrate the theoretical results. We discuss the dynamics behavior of system (3.1). Since the choice of the threshold level N_t is different, system (3.1) will show various dynamics. There are three cases to consider. First, we discretize system (3.1) as follows:

$$\begin{cases} x(j+1) = x(j) + \Delta t(\Lambda - ax(j) - \beta x(j)v(j) - \gamma x(j)y(j)), \\ y(j+1) = y(j) + \Delta t(\beta x(j)v(j) + \gamma x(j)y(j) - by(j) - \varepsilon\mu_1 y(j)), \\ v(j+1) = v(j) + \Delta t(ky(j) - cv(j) - \varepsilon\mu_2 v(j)). \end{cases} \tag{5.1}$$

In Table 1, all parameter values are exhibited. Some values are collected from different papers [6, 17], and others are assumed.

Table 1. Parameter values of numerical experiments for model (2.2).

Parameter	Value	Source of data
Λ	10	[17]
a	0.01	[17]
β	0.00034	Assumed
γ	0.0001	Assumed
b	0.26	[6]
k	11	[6]
c	0.1	[6]
μ_1	0.3	Assumed
μ_2	0.1	Assumed

Case 1: E_1^* is a real equilibrium, and E_2^* is a virtual equilibrium.
This situation is established. Suppose that the following conditions are satisfied:

$$y_1^* < N_t \ \ and \ \ y_2^* < N_t. \tag{5.2}$$

In this case, both equilibriums are located on the same side of the plane N_t, namely, the region G_1. Thus, when (5.2) is satisfied, we obtain that E_1^* can achieve stability. In Figure 1 $E_1^* \in G_1$ achieves stability with $N_t = 60$, and the possible trajectories of this figure are shown: A trajectory that starts in region G_1 will converge to E_1^* as $t \to +\infty$ with hitting and sliding down on the sliding domain $S \subset G_s$; a trajectory of the initial point in region G_2 will cross the manifold G_s, then enter region G_1 and finally converge to E_1^*; a trajectory that begins in region G_1 or G_2 will hit and slide to the boundary of the sliding domain $S \subset G_s$ before moving towards E_1^*.

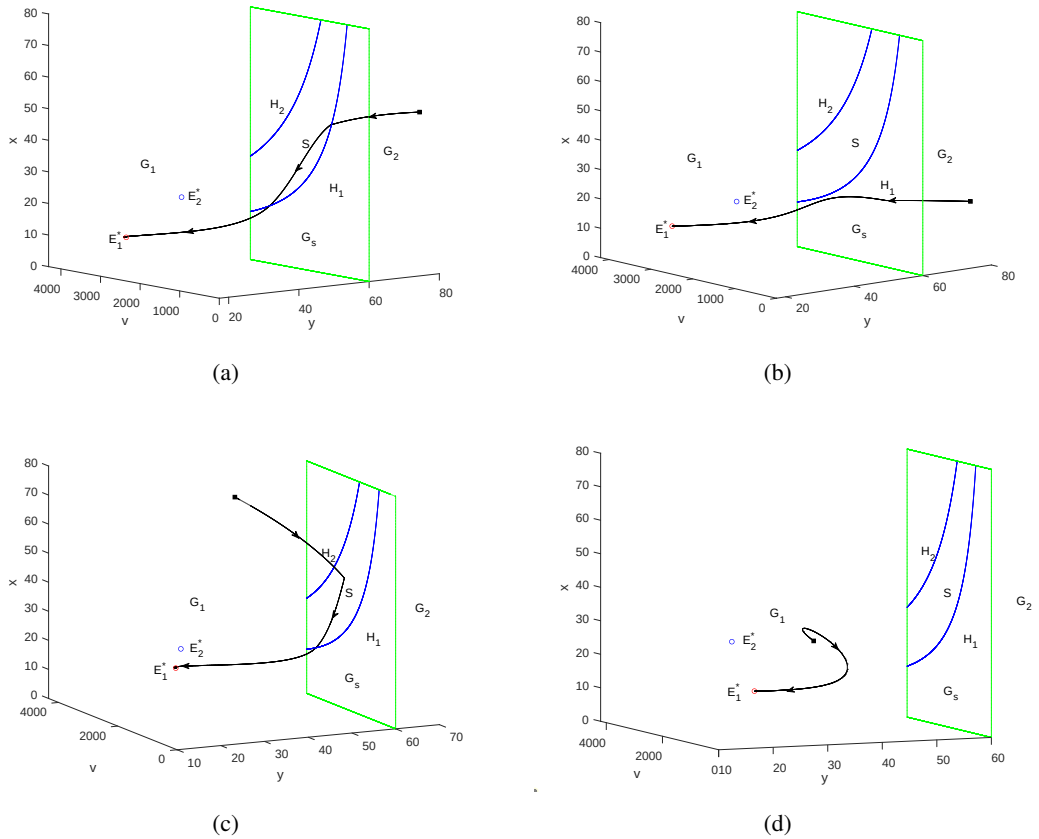

Figure 1. $E_1^* \in G_1$ achieves stability with $N_t = 60$.

Case 2: E_2^* is a real equilibrium, and E_1^* is a virtual equilibrium.
This situation is established. Suppose that the following conditions are satisfied:

$$y_1^* > N_t \ \ and \ \ y_2^* > N_t. \tag{5.3}$$

In this case, both equilibriums are located on the same side of the plane N_t, namely, the region G_2. Thus, when (5.3) is satisfied, we obtain that E_2^* can achieve stability. In Figure 2 $E_2^* \in G_2$ achieves stability with $N_t = 15$, and the possible trajectories of this figure are shown: A trajectory with initial condition in region G_2 will converge to E_2^* as $t \to +\infty$ with hitting and sliding up on the sliding domain $S \subset G_s$; a trajectory with initial point in region G_1 will pass through the manifold G_s from G_1 to G_2; a trajectory that starts in region G_1 or G_2 will hit and slide up on the boundary of the sliding domain $S \subset G_s$ before moving towards E_2^*.

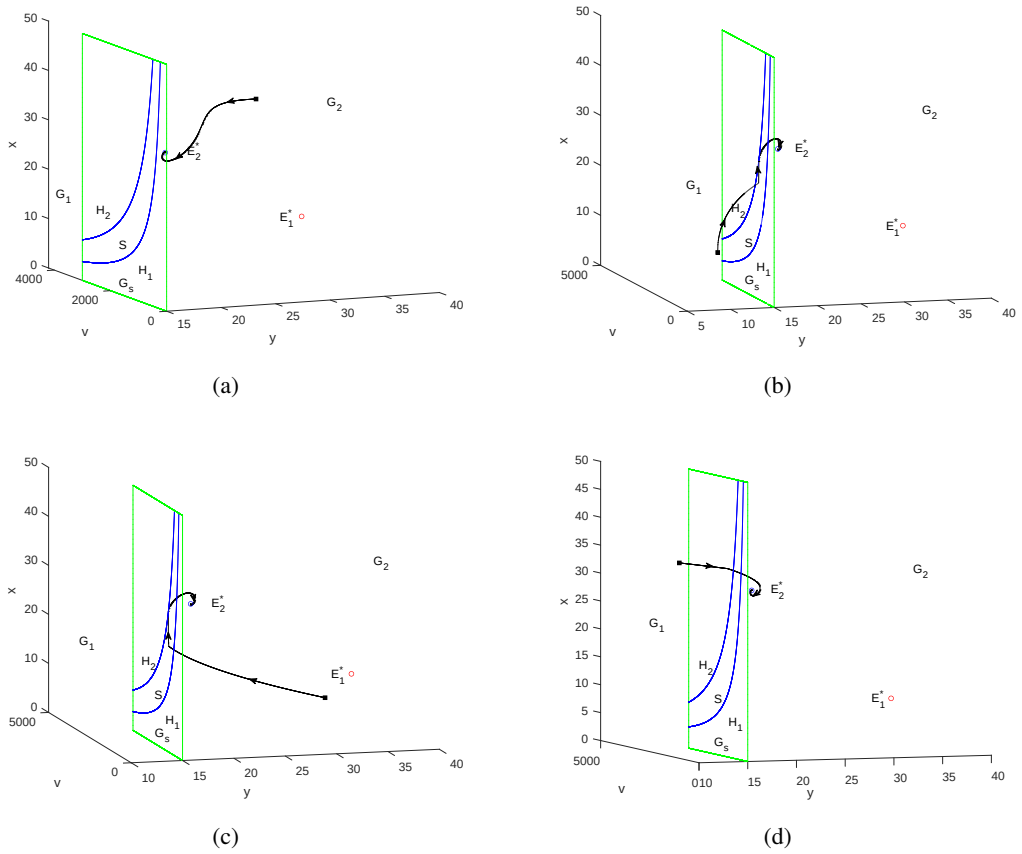

Figure 2. $E_2^* \in G_2$ achieves stability with $N_t = 15$.

Case 3: Both E_1^* and E_2^* are virtual equilibria.
This situation is established. Suppose that the following conditions are satisfied:

$$y_1^* > N_t \ \ and \ \ y_2^* < N_t. \tag{5.4}$$

For this case, we can find that E_1^* and E_2^* belong to regions G_2 and G_1, respectively. If $E_S^* \in S \subset G_s$, it is a pseudo-equilibrium. Thus, when (5.4) is satisfied, we obtain that E_s^* is stable when it exists. Figure 3 $E_s^* \in S$ achieves stability with $N_t = 25$, and the possible trajectories of this figure are shown: A trajectory with initial condition in region G_1 will converge to E_s^* as $t \to +\infty$; a trajectory that begins in region G_2 will cross the manifold G_s, then enter region G_1 and finally converge to E_s^*; a trajectory with initial condition in region G_1 or G_2 will hit and slide down on $S \subset G_s$ before converging to E_s^* .

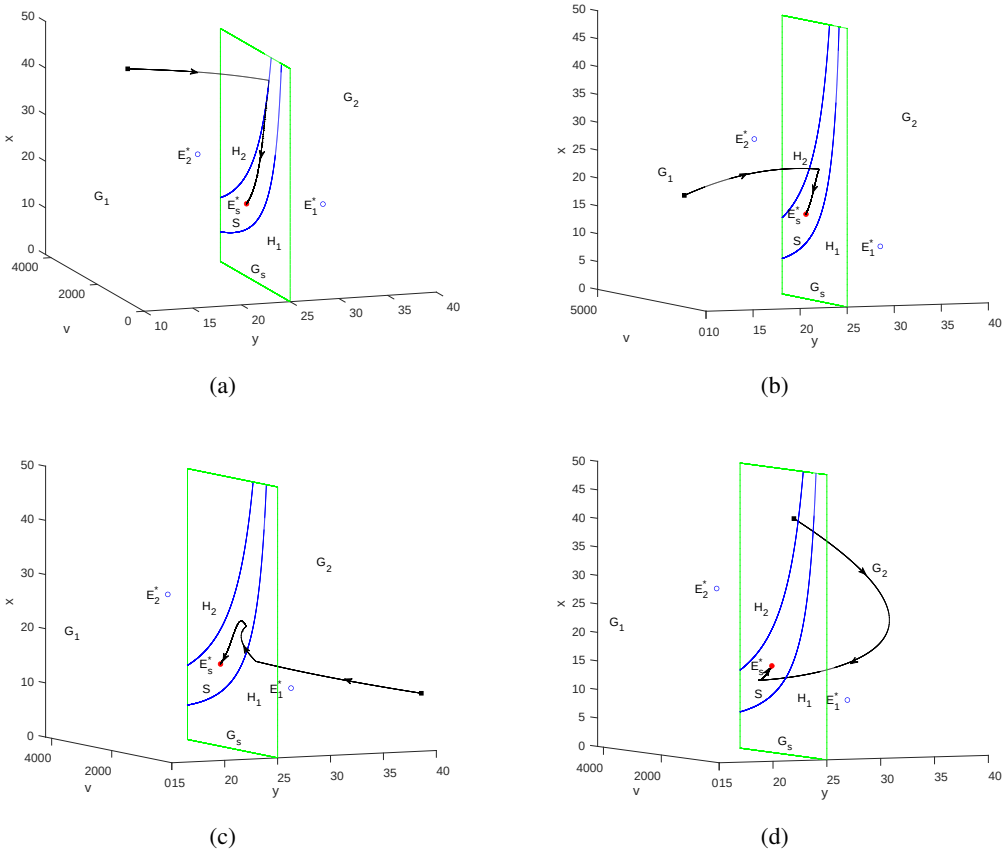

Figure 3. $E_s^* \in S$ achieves stability with $N_t = 25$.

5.2. Numerical simulations of the optimal control

In this subsection, we also discretize the optimal control system (4.1) as

$$\begin{cases} x(j+1) = x(j) + \Delta t(\Lambda - ax(j) - \beta x(j)v(j) - \gamma x(j)y(j)), \\ y(j+1) = y(j) + \Delta t(\beta x(j)v(j) + \gamma x(j)y(j) - by(j) - u_1(j)y(j)), \\ v(j+1) = v(j) + \Delta t(ky(j) - cv(j) - u_2(j)v(j)). \end{cases} \tag{5.5}$$

The parameter values Λ, a, b, β, γ, k and c are chosen as shown in Table 1, and $A_1 = 20, A_2 = 50, A_3 = 0.1, A_4 = 0.1$. Then, we compare the effects of different control intensities by the following figures. The cost of control strategies must be considered, and the cost of each measure is different, so we want to know the change under only one control strategy compared with two control strategies. Thus, we make simulations under only $u_1(t)$ (see Figure 4) or $u_2(t)$ (see Figure 5) and optimal control (see Figure 6).

When initial value $(x_0, y_0, v_0) = (50, 150, 800)$, Figure 4 illustrates that if the control strategy is only applied to infected cells ($u_2(t) = 0$), the concentration of infected cells and viruses will decrease. Meanwhile, the number of infected cells and viruses decreased with the increase of $u_1(t)$ intensity. Figure 5 shows that if the control strategy is only applied to viruses ($u_1(t) = 0$), the density of infected

cells and viruses will also decrease, and the number of infected cells and viruses decreased with the increase of $u_2(t)$ intensity.

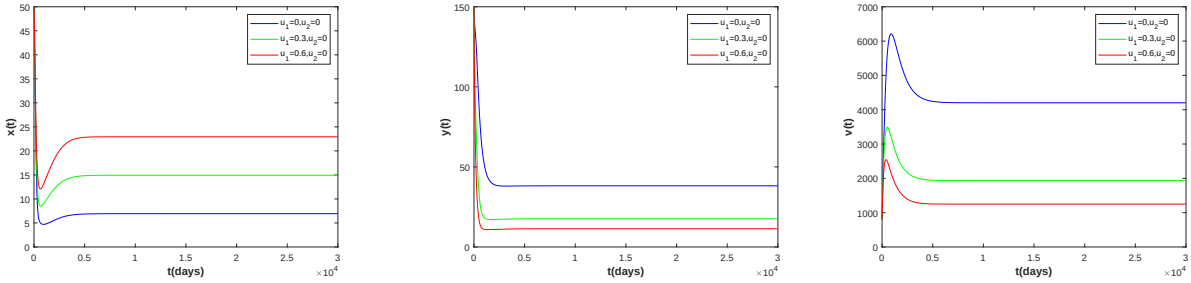

(a) (b) (c)

Figure 4. The states of $x(t), y(t)$ and $v(t)$ when $u_1 = 0, 0.3, 0.6$ and $u_2 = 0, 0, 0$.

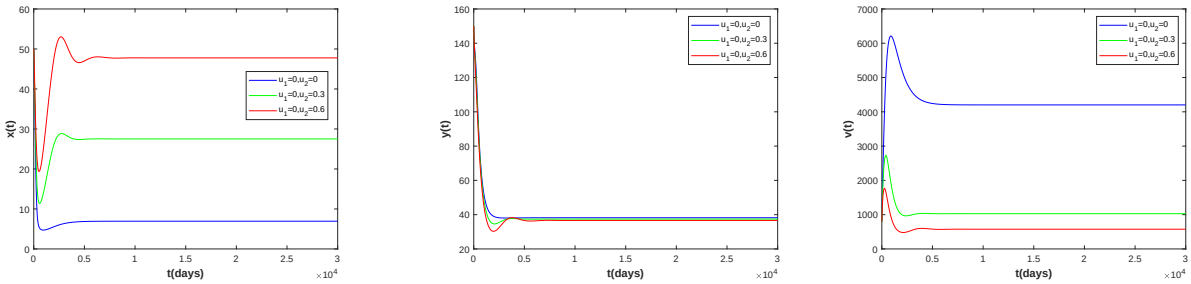

(a) (b) (c)

Figure 5. The states of $x(t), y(t)$ and $v(t)$ when $u_1 = 0, 0, 0$ and $u_2 = 0, 0.3, 0.6$.

The expressions of optimal control $u_1^*(t)$ and $u_2^*(t)$ are obtained through calculation (in Eq (4.27)), and then we obtain the optimal control states of uninfected cells, infected cells and viruses in Figure 6, which shows that the concentration of infected cells and viruses decreases to some extent after the control is applied, and the combination of multi-drug works better than a single-drug approach. Figure 7 shows the values of control variables $u_1(t)$ and $u_2(t)$ in each time. Eventually, the concentration of infected cells and viruses and control intensity gradually decrease and stabilize. Thus, the control strategies in our model have significant influence on the spread of HIV.

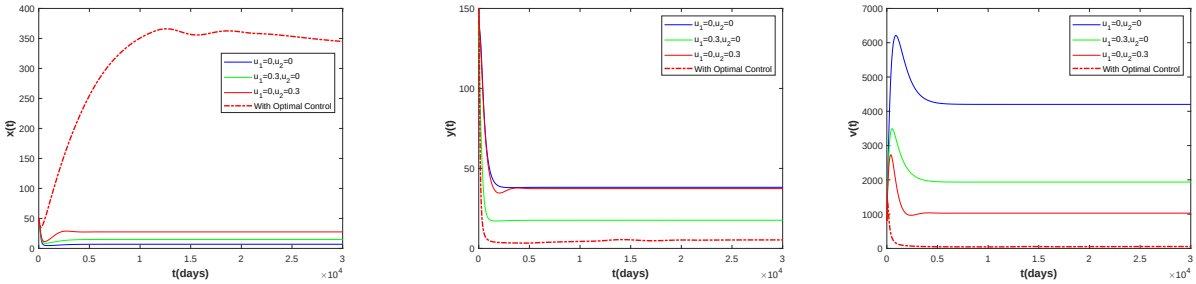

(a) (b) (c)

Figure 6. The paths of $x(t)$, $y(t)$ and $v(t)$ with and without optimal control.

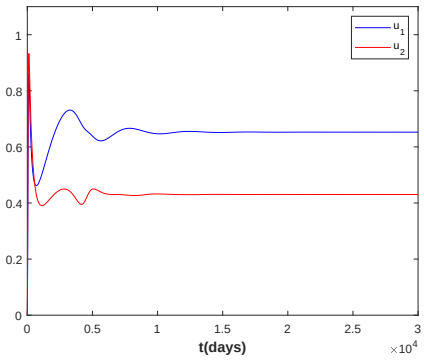

(a)

Figure 7. The path of the two controls.

6. Conclusions and discussion

In this paper, we have proposed an HIV model with cell-to-cell transmission and analyzed the sliding mode dynamics of the model and optimal control problem. First, we extended a novel Filippov model (3.1), which indicates that corresponding control measures (i.e., antiretroviral drugs RTIs and PIs) are triggered once the total number of infected cells reaches the threshold level N_t, where RTIs prevent new HIV infections by blocking the transformation of viral RNA into DNA in T cells, and PIs reduce the number of viral particles produced by actively infected T cells [21]. Further, the sliding domain and sliding mode dynamics of system (2.2) have been examined. In addition, the simulation results show that the model solution is either near a real equilibrium point or near a pseudo-equilibrium point according to the different threshold levels. It is worth mentioning that some parameters can be simulated through actual data, and the basic reproduction number can be calculated to judge the stability. In addition, the number of viruses and infected cells can reduce to a previously desired level when the threshold level is chosen properly. Because different patients have different initial viral loads, an individualized therapy is suggested, which shows that the choice of a treatment strategy for a given patient should depend on HIV viruses and infected cells and proposed threshold level.

Moreover, the cost of treatment is beyond the reach of many infected patients. Therefore, we have introduced an optimal therapy to minimize the cost of treatment and reduce the viral load and the number of infected cells. Then, the efficacies of RTIs and PIs and their combinations have been measured. In addition, we have discussed an efficient numerical method based on optimal control to determine the best treatment strategy for HIV infection. Our results indicate that with the increase of treatment intensity, the number of infected cells and viruses decreases, while the density of $CD4^+T$ increases. Due to the multiple transmission routes of HIV, the combined use of multiple drugs is better than the use of a single drug. From a biological point of view, it can be concluded that optimal control is adopted when the number of infected cells in the patient is higher than threshold level N_t, and at this time, the economic cost can be considered to select the optimal control measures. Control measures are not necessary when the concentration of infected cells is low. Optimal control path is shown in Figure 7.

The results of this paper have practical implications for controlling HIV transmission. However, our work is only a preliminary exploration of the impact of some control measures on HIV transmission, which can be improved in many aspects. The number of viruses in the infected person varies with age, so it is interesting and challenging to consider the sliding mode control of HIV model with age structure. We can also refer to the methods in the literature [33, 34] to study the fractional-order HIV model. These issues will be the focus of our future research.

Acknowledgments

The research was supported by the Key Research and Development Program of Ningxia (2020BEB04007) and the Fundamental Research Funds for the Central Universities, North Minzu University (2020KYQD17).

Conflict of interest

The authors declare there is no conflict of interest.

References

1. D. D. Ho, A. U. Neumann, A. S. Perelson, W. Chen, J. M. Leonard, M. Markowitz, Rapid turnover of plasma virions and CD4 lymphocytes in HIV-1 infection, *Nature*, **373** (1995), 123–126. https://doi.org/10.1038/373123a0

2. T. Doyle, A. M. Geretti, Low-level viraemia on HAART: significance and management, *Curr. Opin. Infect. Dis.*, **25** (2012), 17–25. https://doi.org/10.1097/qco.0b013e32834ef5d9

3. S. Wain-Hobson, Virus dynamics: mathematical principles of immunology and virology, *Nat. Med.*, **7** (2001), 525–526. https://doi.org/10.1038/87836

4. D. M. Cardo, D. H. Culver, C. A. Ciesielski, P. U. Srivatava, R. Marcus, D. Abiteboul, et al., A case-control study of HIV seroconversion in health care workers after percutaneous exposure, *N. Engl. J. Med.*, **337** (1997), 1485–1490. https://doi.org/10.1056/NEJM199711203372101

5. N. K. Vaidya, L. Rong, Modeling pharmacodynamics and hiv latent infection: choice of drugs is key to successful cure via early therapy, *SIAM J. Appl. Math*, **77** (2017), 1781–1804. https://doi.org/10.1137/16m1092003
6. P. K. Roy, *Mathematical Models for Therapeutic Approaches to Control HIV Disease Transmission*, Springer, 2015. https://doi.org/10.1007/978-981-287-852-6
7. P. Yan, Impulsive SUI epidemic model for HIV/AIDS with chronological age and infection age, *J. Theor. Biol.*, **265** (2010), 177–184. https://doi.org/10.1016/j.jtbi.2010.04.011
8. S. B. Chibaya, F. Nyabadza, Mathematical modelling of the potential role of supplementary feeding for people living with HIV/AIDS, *Int. J. Appl. Comput. Math.*, **5** (2019), 1–20. https://doi.org/10.1007/s40819-019-0660-9
9. A. S. Perelson, A. U. Neumann, M. Markowitz, J. M. Leonard, D. D. Ho, HIV-1 dynamics in vivo: Virion clearance rate, infected cell life-span, and viral generation time, *Science*, **271** (1996), 1582–1586. https://doi.org/10.1126/science.271.5255.1582
10. L. Cai, X. Li, M. Ghosh, B. Guo, Stability analysis of an HIV/AIDS epidemic model with treatment, *J. Comput. Appl. Math.*, **229** (2009), 313–323. https://doi.org/10.1016/j.cam.2008.10.067
11. L. M. Agosto, P. D. Uchil, W. Mothes, HIV cell-to-cell transmission: effects on pathogenesis and antiretroviral therapy, *Trends Microbiol.*, **23** (2015), 289–295. https://doi.org/10.1016/j.tim.2015.02.003
12. J. Wang, J. Lang, X. Zou, Analysis of an age structured HIV infection model with virus-to-cell infection and cell-to-cell transmission, *Nonlinear Anal. Real World Appl.*, **34** (2017), 75–96. https://doi.org/10.1016/j.nonrwa.2016.08.001
13. W. H*ü*ebner, G. P. Mcnemey, M. Nerney, P. Chen, B. M. Dale, R. E. Gordon, et al., Quantitative 3D video microscopy of HIV transfer across T cell virological synapses, *Science*, **323** (2009), 1743–1747. https://doi.org/10.1126/science.1167525
14. Q. Sattentau, Avoiding the void: Cell-to-cell spread of human viruses, *Nat. Rev. Microbiol.*, **6** (2008), 815–826. https://doi.org/10.1038/nrmicro1972
15. P. Zhong, L. M. Agosto, J. B. Munro, W. Mothes, Cell-to-cell transmission of viruses, *Curr. Opin. Virol.*, **3** (2013), 44–50. https://doi.org/10.1016/j.coviro.2012.11.004
16. X. Wang, S. Tang, X. Song, L. Rong, Mathematical analysis of an HIV latent infection model including both virus-to-cell infection and cell-to-cell transmission, *J. Biol. Dyn.*, **11** (2017), 455–483. https://doi.org/10.1080/17513758.2016.1242784
17. M. Dhar, S. Samaddar, P. Bhattacharya, Modeling the cell-to-cell transmission dynamics of viral infection under the exposure of non-cytolytic cure, *J. Appl. Math. Comput.*, **65** (2021), 885–911. https://doi.org/10.1007/s12190-020-01420-w
18. N. M. Dixit, A. S. Perelson, Multiplicity of human immunodeficiency virus infections in lymphoid tissue, *J. Virol.*, **78** (2004), 8942–8945. https://doi.org/10.1128/jvi.78.16.8942-8945.2004
19. X. Lai, X. Zou, Modeling HIV-1 virus dynamics with both virus-to-cell infection and cell-to-cell transmission, *SIAM J. Appl. Math.*, **74** (2014), 898–917. https://doi.org/10.1137/130930145

20. N. M. Dixit, A. S. Perelson, HIV dynamics with multiple infections of target cells, *Biophys. Comput. Biol.*, **102** (2005), 8198–8203. https://doi.org/10.1073/pnas.0407498102

21. J. J. Kutch, P. Gurfil, Optimal control of HIV infection with a continuously-mutating viral population, in *Proceedings of the 2002 American Control Conference*, **5** (2002), 4033–4038. https://doi.org/10.1109/acc.2002.1024560

22. Y. Liu, X. Lin, J. Li, Analysis and control of a delayed HIV infection model with cell-to-cell transmission and cytotoxic T lymphocyte immune response, *Math. Methods Appl. Sci.*, **44** (2021), 5767–5786. https://doi.org/10.1002/mma.7147

23. N. Akbari, R. Asheghi, Optimal control of an HIV infection model with logistic growth, celluar and homural immune response, cure rate and cell-to-cell spread, *Boundary Value Probl.*, **2022** (2022), 1–12. https://doi.org/10.1186/s13661-022-01586-1

24. W. Guo, Q. Zhang, X. Li, M. Ye, Finite-time stability and optimal impulsive control for age-structured HIV model with time-varying delay and L*é*vy noise, *Nonlinear Dyn.*, **106** (2021), 3669–3696. https://doi.org/10.1007/s11071-021-06974-3

25. E. Moulay, V. L*é*chapp*é*, E. Bernuau, M. Defoort, F. Plestan, Fixed-time sliding mode control with mismatched disturbances, *Automatica*, **136** (2022), 110009. https://doi.org/10.1016/j.automatica.2021.110009

26. G. Yan, Design of adaptive sliding mode controller applied to ultrasonic motor, *Assem. Autom.*, **42** (2022), 147–154. https://doi.org/10.1108/aa-04-2021-0048

27. L. Shen, S. A. Rabi, A. R. Sedaghat, L. Shan, J. Lai, S. Xing, et al., A critical subset model provides a conceptual basis for the high antiviral activity of major HIV drugs, *Sci. Transl. Med.*, **3** (2011), 63–91. https://doi.org/10.1126/scitranslmed.3002304

28. J. Lou, Y. Lou, J. Wu, Threshold virus dynamics with impulsive antiretroviral drug effects, *J. Math. Biol.*, **65** (2012), 623–652. https://doi.org/10.1007/s00285-011-0474-9

29. S. Chibaya, M. Kgosimore, E. S. Massawe, Mathematical analysis of drug resistance in vertical transmission of HIV/AIDS, *Open J. Epidemiol.*, **3** (2013), 139–148. https://doi.org/10.4236/ojepi.2013.33021

30. R. Mu, A. Wei, Y. Yang, Global dynamics and sliding motion in A(H7N9) epidemic models with limited resources and Filippov control, *J. Math. Anal. Appl.*, **477** (2019), 1297–1317. https://doi.org/10.1016/j.jmaa.2019.05.013

31. V. L. Utikin, J. Guldner, J. Shi, *Sliding Mode Control in Electro-Mechanical Systems*, CRC Press, 2009. https://doi.org/10.1201/9781420065619

32. J. Yong, X. Zhou, *Stochastic Controls: Hamiltonian Systems and HJB Equations*, Springer, 1999. https://doi.org/10.1109/TAC.2001.964706

33. C. Xu, W. Zhang, Z. Liu, L. Yao, Delay-induced periodic oscillation for fractional-order neural networks with mixed delays, *Neurocomputing*, **488** (2022), 681–693. https://doi.org/10.1016/j.neucom.2021.11.079

34. C. Xu, D. Mu, Z. Liu, Y, Pang, M. Liao, P. Li, et al., Comparative exploration on bifurcation behavior for integer-order and fractional-order delayed BAM neural networks, *Nonlinear Anal. Modell. Control*, **27** (2022), 1–24. https://doi.org/10.15388/namc.2022.27.28491

AIMS Press